Supporting Materials

MicroRNA-223 ameliorates nonalcoholic steatohepatitis and cancer by targeting multiple inflammatory and oncogenic genes in hepatocytes

Yong He, Seonghwan Hwang, Yan Cai, Seung-Jin Kim, Mingjiang Xu, Dingcheng Yang, Adrien Guillot, Dechun Feng, Wonhyo Seo, Xin Hou, Bin Gao*

Laboratory of Liver Diseases, National Institute on Alcohol Abuse and Alcoholism, National Institutes of Health, Bethesda, MD, 20892, USA

Methods and Materials

Biochemical assays and Complete blood count (CBC) test: Serum alanine aminotransferase (ALT) levels were determined using a Catalyst Dx Chemistry Analyzer (IDEXX Laboratories, Westbrook, ME). Mouse anticoagulated blood was collected from mice. CBC test was performed with Hemavet 950 FS Hematology Analyzer (Drew Scientific, Dallas, TX)

Tissue processing, Histological analysis, and immunohistochemistry: Formalin-fixed liver samples were processed, and 4-μm–thick paraffin sections were stained with hematoxylin and eosin (H&E) for histological analysis or Sirius Red (collagen/fibrosis) dyes or Masson's trichrome using Masson Trichrome stain kit (sigma, St. Louis, MO). Frozen liver tissues were cryostat sectioned at 10 μm thick and stained with Oil Red O (neutral lipid stain). For immunohistochemistry, after heat-induced epitope retrieval, paraffin-embedded sections were incubated in 3% H_2O_2, and blocked by another 60 mins in 3% normal serum buffer. Sections were incubated with primary antibodies overnight at 4°C. Vectastain Elite ABC Staining Kit and DAB Peroxidase Substrate Kit (Vector

Laboratories, Inc., Burlingame, CA) were used to visualize the staining according to the manufacturer's instructions. Primary antibodies used were listed below: anti-myeloperoxidase (MPO) antibody (Biocare Medical, LLC, Concord, CA), anti-malonaldehyde (MDA) (Genox, Baltimore, MD), 4-hydroxynonenal (4-HNE) (Genox, Baltimore, MD), anti-F4/80 antibody (Cell Signaling Technology, US), anti-CXCL10 antibody (Abcam, Cambridge, MA), anti-CD3 antibody (Novus Biologicals, CO) anti-TAZ antibody (Sigma-Aldrich). The images were taken with an Olympus camera DP72. The positive cells and in 10 randomly selected high-power fields were calculated and analyzed. The percentage of positive area was determined with ImageJ software (National Institutes of Health, Bethesda, MD).

Microarray analyses of mouse liver samples

Total RNAs were isolated from liver tissues of 3-month HFD-fed WT and miR-223KO mice. For each sample, 10 μg total RNA was used for complementary DNA (cDNA) synthesis (SuperScript Double- Stranded cDNA Synthesis Kit; Thermo Fisher Scientific, Inc, Waltham, MA) and coupled with dye. A MiniElute polymerase chain reaction (PCR) purification kit (Qiagen, Germantown, MD) was used to purify dye-coupled cDNAs. The cDNA then was hybridized to an Agilent 44K mouse 60-meroligo microarray (Agilent Technologies, Santa Clara, CA). The data were analyzed with the Genespring GX software package (Agilent Technologies). Ingenuity Pathway Analysis was used to process 5 interactive Venn diagrams and gene function analyses. Full microarray data have been uploaded to NCBI's Gene Expression Omnibus.

Isolation and culture of mouse primary hepatocytes and hepatic stellate cells (HSCs): For hepatocyte and HSC isolation, mice were anesthetized with 30 mg/kg pentobarbital sodium intraperitoneally. Portal vein was cannulated and perfused with Ethylene glycol tetraacetic acid (EGTA) and digested with 0.075% collagenase as described previously.(1) Primary hepatocytes were collected after centrifugation at 400g for 5 min. The mouse hepatocytes were cultured in Dulbecco's modified Eagle's medium (DMEM) containing 10% fetal calf serum and 2 mmol/L penicillin streptomycin.

For HSC isolation, after removing the hepatocytes as described above, the supernatant was transferred to a new tube and recentrifuged at 400g for 10 min at 4°C. The cell pellet was then resuspended in 5 ml of 15%OptiPrep, and loaded carefully with 5 ml of 11.5%OptiPrep, and centrifuged at 1400g for 17 min at 4°C. The cell fraction in the GBSS and 11.5%OptiPrep interphase was gently aspirated, mixed with GBSS. The final cell pellet was collected after centrifuging at 1400g for 10 min at 4°C. The mouse HSCs were cultured in Dulbecco's modified Eagle's medium (DMEM) containing 10% fetal calf serum and 2 mmol/L penicillin streptomycin for 1 day and 5 days.

***Total RNA isolation and real-time quantitative PCR (*RT-qPCR):** Total RNA was purified from liver tissues or cell samples using TRIzol reagents (Invitrogen, Carlsbad, CA) according to the manufacturer's instructions. One microgram of RNA was reverse-transcribed into cDNA using a High-capacity cDNA Reverse Transcription kit (Invitrogen, Carlsbad, CA). The expression levels of mRNA were measured by RT-qPCR with an ABI7500 real-time PCR detection system (Applied Biosystems, Foster City, CA). The mRNA levels of 18s or β-actin were used as an internal control. Each test was done in triple replication and the $2^{-\Delta\Delta Ct}$ method was used to calculate the expression of mRNA. The primers used for real-time PCR are listed in Supporting Table S2.

For miRNA detection, total RNA was isolated from liver tissues and neutrophils by using TRIzol reagents (Invitrogen, Carlsbad, CA), and then the mature miRNA strand cDNA was synthesized using TaqMan® MicroRNA Reverse Transcription Kit (Invitrogen, Carlsbad, CA) according to the manufacturer's instructions. MiRNA was amplified by using TaqMan® MicroRNA Assays (Invitrogen) and TaqMan® Universal PCR Master Mix (Invitrogen) according to the manufacturer's instructions. The fold-change for miRNA relative to snoRNA202 or spiked-in cel-miR-39 was determined by the formula $2^{-\Delta\Delta Ct}$.

Luciferase activity assay

The AML12 cells were cultured in 48-well plates 24h prior to transfection, and then cotransfected with 250 ng Control luciferase vector or CXCL10 and TAZ 3′-UTR luciferase vector plasmid (GeneCopoeia, USA) by using Lipofectamine™ 3000 (Invitrogen), 20 nM miR-223 mimics or the negative controls by using Lipofectamine RNAiMAX Reagent

(Invitrogen) according to the manufacturer's instructions. The Firefly and Renilla luciferase activities were measured using the Luc-Pair™ Duo-Luciferase Assay Kit 2.0 (GeneCopoeia, USA) 48h after transfection as described by the manufacturer. The ratio of luminescence from the Firefly luciferase to the Renilla luciferase was calculated as the relative luciferase activity.

Flow cytometry analysis

Liver tissues were passed through a 70 μm cell strainer in PBS and the cell suspension was centrifuged at 50g for 5 minutes to pellet the hepatocytes. The supernatant enriched liver leukocytes were centrifuged at 1600 rmp for 10 minutes. The pellet was resuspended in 15 ml of 40% Percoll (GE Healthcare, Pittsburgh, PA) and centrifuged at 2400 rmp for 15 minutes. The resulting pellet containing leukocytes was resuspended in 2 ml of ACK lysing buffer (BioWhittaker, Walker sville, MD). Cells were then stained with antibodies of interest for 30 minutes at 4°C in the dark. The following antibodies were used: anti-CD45 (BD Biosciences), anti-CD3 (BD Biosciences), anti-CD19 (BD Biosciences), and anti-NK1.1 (BD Biosciences). Flow cytometry analysis was performed using a FACSCalibur (Beckman). Percentage of positive cells in $CD45^+$ lymphocytes was calculated.

Western blotting

Liver tissues and cells were homogenized or lysed in RIPA buffer containing a cocktail of protease inhibitors (Santa Cruz, CA) according to the manufacturer's instruction. Protein extracts were loaded onto 12% acrylamide gels (Bio-Rad) and transferred onto nitrocellulose membranes. Protein bands were visualized with ECL-chemiluminescent kit (GE Healthcare, Piscataway, NJ) or enhanced fluorescence. The antibodies (Abs) against COL1α1, COL3α1, Vimentin, p-JNK, JNK, PCNA, CCND1, CCNE1, YAP, TAZ, p-mTOR and mTOR were purchased from Cell Signaling Technology (Danvers, MA). The Abs against β-actin and α-SMA were purchased from Abcam (Cambridge, MA). The Abs against GPC3 and GOLM1 were purchased from Novus Biologicals (Centennial, CO).

CXCL10 ELISA

The serum levels of mouse CXCL10 were measured by using CXCL10 ELISA kit (Abcam, Cambridge, MA) according to the manufacturer's protocol.

Cell culture and transient transfection of miR-223 mimics

Mouse hepatocyte cell line AML12 cells were cultured in a 1:1 mixture of Dulbecco's modified Eagle's medium and Ham's F12 medium with 0.005 mg/ml insulin, 0.005 mg/ml transferrin, 5 ng/ml selenium, and 40 ng/ml dexamethasone, 10% fetal bovine serum. AML12 cells were transfected with nonspecific miRNA mimics (NS-miRNA) and miR-223 mimics (Thermo fisher Scientific) by Lipofectamine RNAiMAX Reagent (Thermo fisher Scientific) according to the manufacturer's instructions at a final concentration of 10 nM for 24h. After 24h, the cells were stimulated with Palmitic acid (PA) (Cayman, Ann Arbor, Michigan) for the indicated time. The PA was conjugated to free fatty acid (FFA)-free bovine serum albumin (BSA, Sigma-Aldrich) by adding FFAs to 10% BSA-Tris buffer (pH 8.0) and shaking over-night at 37ºC. The final FFA concentration was 8 mM with the ratio of 5:1 for PA to BSA.

References:

1. Chang B, Xu MJ, Zhou Z, Cai Y, Li M, Wang W, Feng D, et al. Short- or long-term high-fat diet feeding plus acute ethanol binge synergistically induce acute liver injury in mice: an important role for CXCL1. Hepatology 2015;62:1070-1085.

Supporting Table S1. The list general characteristics of the normal and NASH human liver samples.

Normal		
#	**Gender**	**Age**
1	M	46
2	M	64
3	F	49
4	F	62
5	M	48
6	M	29
7	M	24
8	M	48
9	F	63
10	M	28

NASH			
#	**Gender**	**Age**	**Primary Diagnosis**
1	M	16	Fatty liver, 50% fat was estimated in the liver
2	F	62	Fatty liver, cirrhosis
3	F	59.2	Fatty liver, cirrhosis secondary to steatohepatitis
4	F	58.6	Fatty liver, diagnosed as NASH
5	F	57.2	Fatty liver, cirrhosis
6	M	62.3	Fatty liver, secondary to NASH
7	F	43.5	Fatty liver, diagnosed as NASH
8	F	55.3	Fatty liver, secondary to NASH, cirrhosis
9	F	62	Fatty liver, NASH
10	F	48.3	Fatty liver, cirrhosis
11	F	67.6	Cryptogenic Cirrhosis/ NASH
12	F	63	NASH – fatty, Cirrhosis secondary to NASH
13	M	68.5	Cirrhosis secondary to NASH, HCC/ NASH - no longer fatty
14	F	58.7	NASH, cirrhosis.

Supporting Table S2: RT-qPCR primer sequences

Genes (mouse)	Forward primer (5′–3′)	Reverse primer (5′–3′)
Tnfα	AGGCTGCCCCGACTACGT	GACTTTCTCCTGGTATGAGATAGCAAA
Il6	TCCATCCAGTTGCCTTCTTG	TTCCACGATTTCCCAGAGAAC
Il10	CCAAGCCTTATCGGAAATGA	TTTTCACAGGGGAGAAATCG
Ly6g	TGCGTTGCTCTGGAGATAGA	CAGAGTAGTGGGGCAGATGG
F4/80	GGAAAGCACCATGTTAGCTGC	CCTCTGGCTGCCAAGTTAATG
Mcp1	CCAGCCTACTCATTGGGAT	GGGCCTGCTGTTCACAGTT
Mip1α	TGAGAGTCTTGGAGGCAGCGA	TGTGGCTACTTGGCAGCAAACA
Mip1β	AACACCATGAAGCTCTGCGT	AGAAACAGCAGGAAGTGGGA
Mip2	TCCAGGTCAGTTAGCCTTGC	CGGTCAAAAAGTTTGCCTTG
Icam-1	CAATTTCTCATGCCGCACAG	AGCTGGAAGATCGAAAGTCCG
Srebp1c	GGCTCTGGAACAGACACTGG	TGGTTGTTGATGAGCTGGAG
Scd-1	TTCTTGCGATACACTCTGGTGC	CGGGATTGAATGTTCTTGTCGT
Acc-1	GATGAACCATCTCCGTTGGC	GACCCAATTATGAATCGGGAGTG
Cidea	TCTGCAATCCCATGAATGTC	CAGTGATTTAAGAGACGCGG
Cideb	ACGTAGCAGCAAGGTCTCCA	GACCCTTCCGTGTCTGTGAT
Fas	GGAGGTGGTGATAGCCGGTAT	TGGGTAATCCATAGAGCCCAG
Cpt-1	GCACACCAGGCAGTAGCTTT	CAGGAGTTGATTCCAGACAGGTA
Pparγ	GATGCACTGCCTATGAGCAC	TCTTCCATCACGGAGAGGTC
α-sma	TCCTGACGCTGAAGTATCCGATA	GGTGCCAGATCTTTTCCATGTC
Col1α1	TAGGCCATTGTGTATGCAGC	ACATGTTCAGCTTTGTGGACC
Col1α2	GGTGAGCCTGGTCAAACGG	ACTGTGTCCTTTCACGCCTTT
Col3α1	TAGGACTGACCAAGGTGGCT	GGAACCTGGTTTCTTCTCACC
Mmp-13	CTTTGGCTTAGAGGTGACTGG	AGGCACTCCACATCTTGGTTT
Vimentin	TCCACTTTCCGTTCAAGGTC	AGAGAGAGGAAGCCGAAAGC
Cxcl9	CGATCCACTACAAATCCCTCA	TAGGCAGGTTTGATCTCCGT
Cxcl10	CTCATCCTGCTGGGTCTGAG	CCTATGGCCCTCATTCTCAC
Cxcl11	CCACAGCTGCTCAAGGCTTC	AACTTTGTCGCAGCCGTTAC
Cxcr3	TCTCGTTTTCCCCATAATCG	AGCCAAGCCATGTACCTTGA
Pcna	GGAGACAGTGGAGTGGCTTT	TGGATAAAGAAGAGGAGGCG
Ki67	GACAGCTTCCAAAGCTCACC	TGTGTCCTTAGCTGCCTCCT
Afp	CAGCAGCCTGAGAGTCCATA	GGCGATGGGTGTTTAGAAAG
Gpc3	TGGTGTAGTTCTTGGCATGG	TGCTCCAGTCTGCGAGTATG
Golm	GCAGGTCTCGAATGAGCTTC	CCAGTCTAGCCACAGCTTCC
Ccnb1	GGCTTGGAGAGGGATTATCA	ACCAGAGGTGGAACTTGCTG
Ccnb2	CAGAGAAAGCTTGGCAGAGG	TGAAACCAGTGCAGATGGAG
Ccnd1	GCGTACCCTGACACCAATCTC	CTCCTCTTCGCACTTCTGCTC
Ccne1	TCCACGCATGCTGAATTATC	TTGCAAGACCCAGATGAAGA
Serpinb9	GACACATCATCTGCACTGGC	AAGGAAAGTGGCATCAACCA
Nrxn1	AGTCACAGCTGAAGCCATCC	ATGGGCAAATTGAGAGAGGA
Slc1a4	GCAACCACAAGATTGGAAGG	CTGGAGAACTCAGGGCCTC
Slc16a6	CTCCATCAGGCACTTGGGTA	GGTGCCTTTTGGGGTTTATT
Dock11	GCCATTGGCAAGTTCAGAG	GGATCCTAAGGTTCTTGCTGA
Wwtr1/Taz	CATGGCGGAAAAAGATCCTCC	GTCGGTCACGTCATAGGACTG
Keratin 8	GAGGAGAGCAGGCTGGAGTC	GCTTCCCATCTCGGGTTTCA
Keratin 18	CCTCAATCTGCTGAGACCAGTA	CTGTGGAGAGCGACATCCAT
18s	AACTTTCGATGGTAGTCGCCGT	TCCTTGGATGTGGTAGCCGTTT

Genes (human)	Forward primer (5′–3′)	Reverse primer (5′–3′)
IL6	GTCAGGGGTGGTTTATTGCA	AGTGAGGAACAAGCCAGAGC
MCP1	AGGTGACTGGGGCATTGAT	GCCTCCAGCATGAAAGTCTC
MIP1A	TGAAATTCTGTGGAATCTGCC	GGCTCTCTGCAACCAGTTCT
MIP1β	GCTTGCTTCTTTTGGTTTGG	CTTTTCTTACACCGCGAGGA
A-SMA	GTGACGAAGCACAGAGCAAA	CTTTTCCATGTCGTCCCAGT
COL1A1	CAGATCACGTCATCGCACAA	TGTGAGGCCACGCATGAG
COL3A1	AGGACTGACCAAGATGGGAA	AGGGGAGCTGGCTACTTCTC
COL4A1	CCTTTTGTCCCTTCACTCCA	CTCCACGAGGAGCACAGC
CXCL10	GAATCGAAGGCCATCAAGAA	CCTCTGTGTGGTCCATCCTT
WWTR1/TAZ	TCCCAGCCAAATCTCGTGATG	AGCGCATTGGGCATACTCAT
SERPINB9	GTTGTTGCCGGGTAGCTCAAT	CAAACGGTTCATTCCACTTTCC
NRXN1	TAAGTGGCCTCCTAATGACCG	TCGCACCAATACGGCTTCTTT
DOCK11	ACACTGTGCAGAACCCTATATCA	ACACTTGTTTAGCTGTCCTGTG
SLC1A4	CAGCGACCCTTCCCTCTATGA	GCCCCGATGGGGAGAATAAAC
SLC16A6	TTGGCAAAAGACGTTCCATAGT	CTGGTGCGAAAGCAAACACA
NLRP3	GATCTTCGCTGCGATCAACAG	CGTGCATTATCTGAACCCCAC
MEF2C	CTGGTGTAACACATCGACCTC	GATTGCCATACCCGTTCCCT
IGF1R	AGGATATTGGGCTTTACAACCTG	GAGGTAACAGAGGTCAGCATTTT
STMN1	TCAGCCCTCGGTCAAAAGAAT	TTCTCGTGCTCTCGTTTCTCA
GPC3	ATTGGCAAGTTATGTGCCCAT	TTCGGCTGGATAAGGTTTCTTC
GOLM1	GTGTGAGGAGCGAATAGAAGAGG	GTCTCTGGTCGTTGTTTTCACT
18S	GGCCCTGTAATTGGAATGAGTC	CCAAGATCCAACTACGAGCTT

Supporting Table S3: Ingenuity Pathway Analysis of HFD-fed WT and miR-223KO microarray data

INGENUITY
PATHWAY ANALYSIS

Analysis Name: IPA GENE LIST FC2 685 - 2017-04-19 04:05 PM
Analysis Creation Date: 2017-04-19
Build version: 439932M
Content version: 33559992 (Release Date: 2017-03-28)

Analysis Settings

Reference set: Whole Mouse Genome Microarray 4x44K v2
Relationship to include: Direct and Indirect
Includes Endogenous Chemicals
Optional Analyses: My Pathways My List

Filter Summary:
Consider only relationships where
confidence = Experimentally Observed

Top Canonical Pathways

Name	p-value	Overlap
B Cell Development	3.43E-03	16.7 % 4/24
Semaphorin Signaling in Neurons	1.12E-02	9.8 % 5/51
Allograft Rejection Signaling	2.49E-02	9.5 % 4/42
Alanine Biosynthesis III	2.66E-02	100.0 % 1/1
Rac Signaling	3.38E-02	6.1 % 7/115

Top Upstream Regulators

Upstream Regulator	p-value of overlap	Predicted Activation
nonylphenol	4.32E-05	
GPD1	1.51E-04	
SLC25A13	1.65E-04	
EOMES	2.92E-04	
EHMT2	3.72E-04	

Top Diseases and Bio Functions

Diseases and Disorders

Name	p-value	#Molecules
Cancer	2.66E-02 - 6.67E-05	390
Organismal Injury and Abnormalities	2.66E-02 - 6.67E-05	397
Reproductive System Disease	2.66E-02 - 6.67E-05	179
Inflammatory Response	2.66E-02 - 8.57E-05	57
Developmental Disorder	2.66E-02 - 1.79E-04	62

Molecular and Cellular Functions

Name	p-value	#Molecules
Cell-To-Cell Signaling and Interaction	2.66E-02 - 8.57E-05	79
Cell Cycle	2.66E-02 - 6.46E-04	20
Cellular Development	2.66E-02 - 7.05E-04	68
Cellular Growth and Proliferation	2.66E-02 - 7.05E-04	66
Molecular Transport	2.66E-02 - 7.05E-04	35

Physiological System Development and Function

Name	p-value	#Molecules
Hematological System Development and Function	2.66E-02 - 8.57E-05	76
Immune Cell Trafficking	2.66E-02 - 8.57E-05	52
Digestive System Development and Function	2.66E-02 - 1.41E-04	18
Embryonic Development	2.66E-02 - 1.41E-04	69
Organismal Development	2.66E-02 - 1.41E-04	78

Top Tox Functions

Assays: Clinical Chemistry and Hematology

Name	p-value	#Molecules
Increased Levels of Albumin	9.85E-03 - 9.85E-03	2
Decreased Levels of Hematocrit	2.24E-02 - 2.24E-02	2
Increased Levels of Potassium	3.68E-01 - 5.24E-02	2
Decreased Levels of Albumin	1.26E-01 - 1.26E-01	1
Decreased Levels of Potassium	1.51E-01 - 1.51E-01	2

Cardiotoxicity

Name	p-value	#Molecules
Cardiac Arrythmia	6.00E-01 - 2.66E-02	11
Cardiac Dilation	2.48E-01 - 2.66E-02	9
Cardiac Hyperplasia/Hyperproliferation	2.66E-02 - 2.66E-02	1
Cardiac Dysfunction	2.96E-01 - 3.74E-02	7
Cardiac Enlargement	5.37E-01 - 4.85E-02	12

Hepatotoxicity

Name	p-value	#Molecules
Liver Hyperplasia/Hyperproliferation	5.04E-01 - 1.44E-02	175
Liver Damage	5.78E-01 - 2.66E-02	12
Liver Inflammation/Hepatitis	5.89E-01 - 2.66E-02	12
Liver Cirrhosis	2.46E-01 - 3.70E-02	11
Liver Cholestasis	1.49E-01 - 1.49E-01	1

Nephrotoxicity

Name	p-value	#Molecules
Renal Damage	4.01E-01 - 1.82E-03	13
Renal Necrosis/Cell Death	5.27E-01 - 8.97E-03	22
Nephrosis	5.38E-01 - 1.35E-02	3
Glomerular Injury	1.00E00 - 2.66E-02	6
Renal Inflammation	5.28E-01 - 2.66E-02	7

Top Networks

ID	Associated Network Functions	Score
1	Cancer, Cell Death and Survival, Organismal Injury and Abnormalities	37
2	Cell-To-Cell Signaling and Interaction, Cellular Assembly and Organization, Cellular Function and Maintenance	37

3	Developmental Disorder, Hereditary Disorder, Neurological Disease	35
4	Lipid Metabolism, Small Molecule Biochemistry, Vitamin and Mineral Metabolism	35
5	Cellular Assembly and Organization, Nervous System Development and Function, Cell Death and Survival	35

Top Tox Lists

Name	p-value	Overlap
Genes Downregulated in Response to Chronic Renal Failure (Rat)	1.95E-03	30.0 % 3/10
Increases Renal Damage	6.98E-03	8.3 % 7/84
Renal Necrosis/Cell Death	1.86E-02	4.3 % 22/511
Reversible Glomerulonephritis Biomarker Panel (Rat)	2.23E-02	13.0 % 3/23
Cytochrome P450 Panel - Substrate is a Xenobiotic (Mouse)	2.49E-02	12.5 % 3/24

Top Analysis-Ready Molecules

Expr Fold Change up-regulated

Molecules	Expr. Value	Expr. Chart
CTSE	↑ 8.737	
Ren2	↑ 6.619	
REN*	↑ 6.028	
BC057193	↑ 4.389	
HSPA1A/HSPA1B*	↑ 4.145	
DYNLT1	↑ 4.126	
SYBU	↑ 3.939	
TMEM209	↑ 3.771	
LRRC39	↑ 3.731	
PIP4K2A	↑ 3.654	

Expr Fold Change down-regulated

Molecules	Expr. Value	Expr. Chart
Hsd3b4 (includes others)	-8.154	
BRD8	-5.089	
Slco1a1*	-4.796	
CRMP1	-4.478	
GP9	-4.402	
POP4	-3.938	
KCNJ3	-3.855	
UNC13A	-3.765	
GJA3	-3.724	
USP53	-3.618	

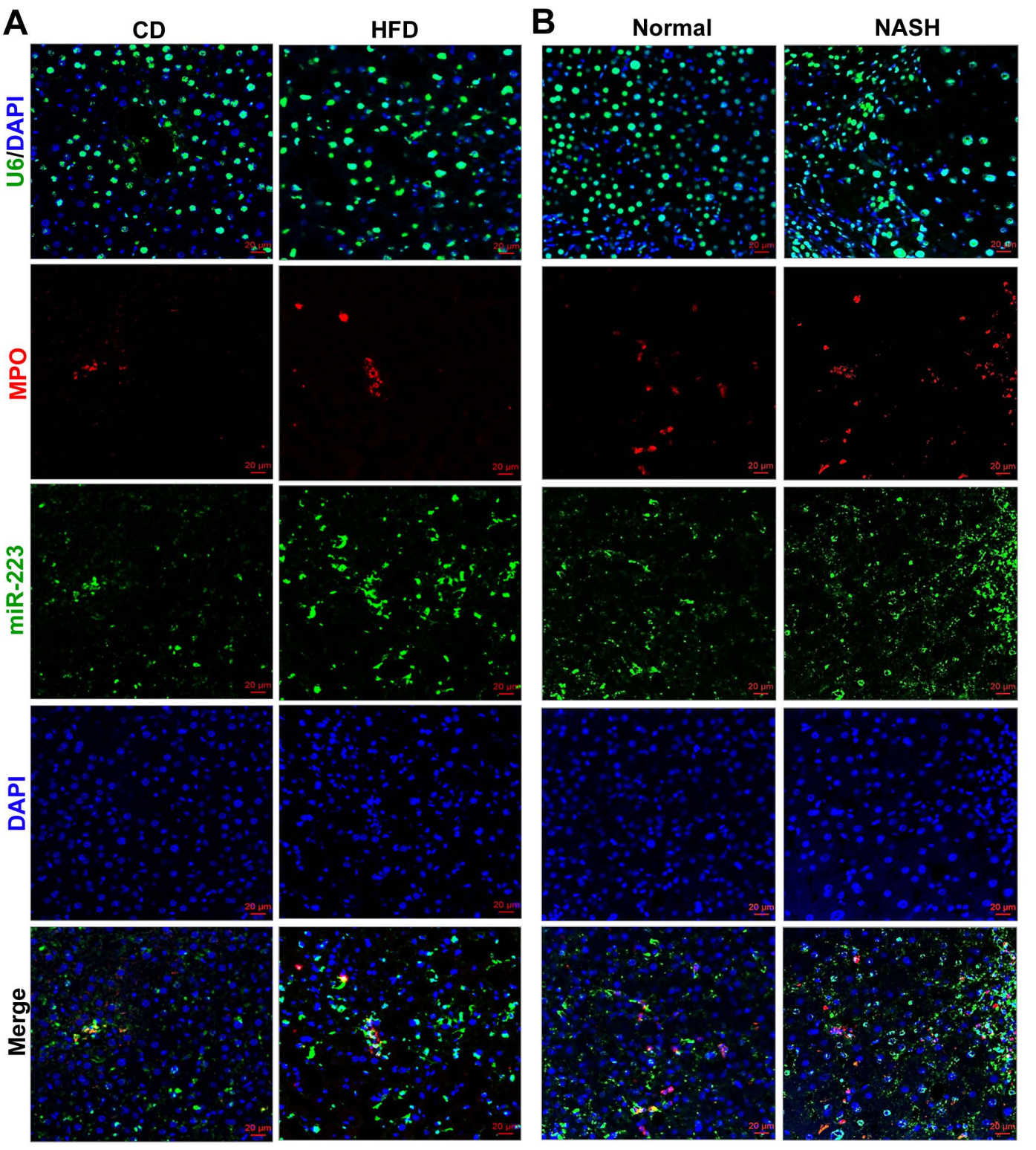

Supporting Fig. S1. miR-223 is highly elevated in the liver from HFD-fed mice and human NASH patients. Liver tissue sections from 3-month CD or HFD-fed mice, or from normal or NASH human livers were subjected to miR-223 In Situ Hybridization along with immunofluorescence staining of neutrophil marker MPO. Representative images of miR-223 or U6 expression (green), MPO (red) and nuclei (blue) were shown. Mouse liver samples were from the frozen tissues (A), while human liver samples were from formalin-fixed tissues (B).

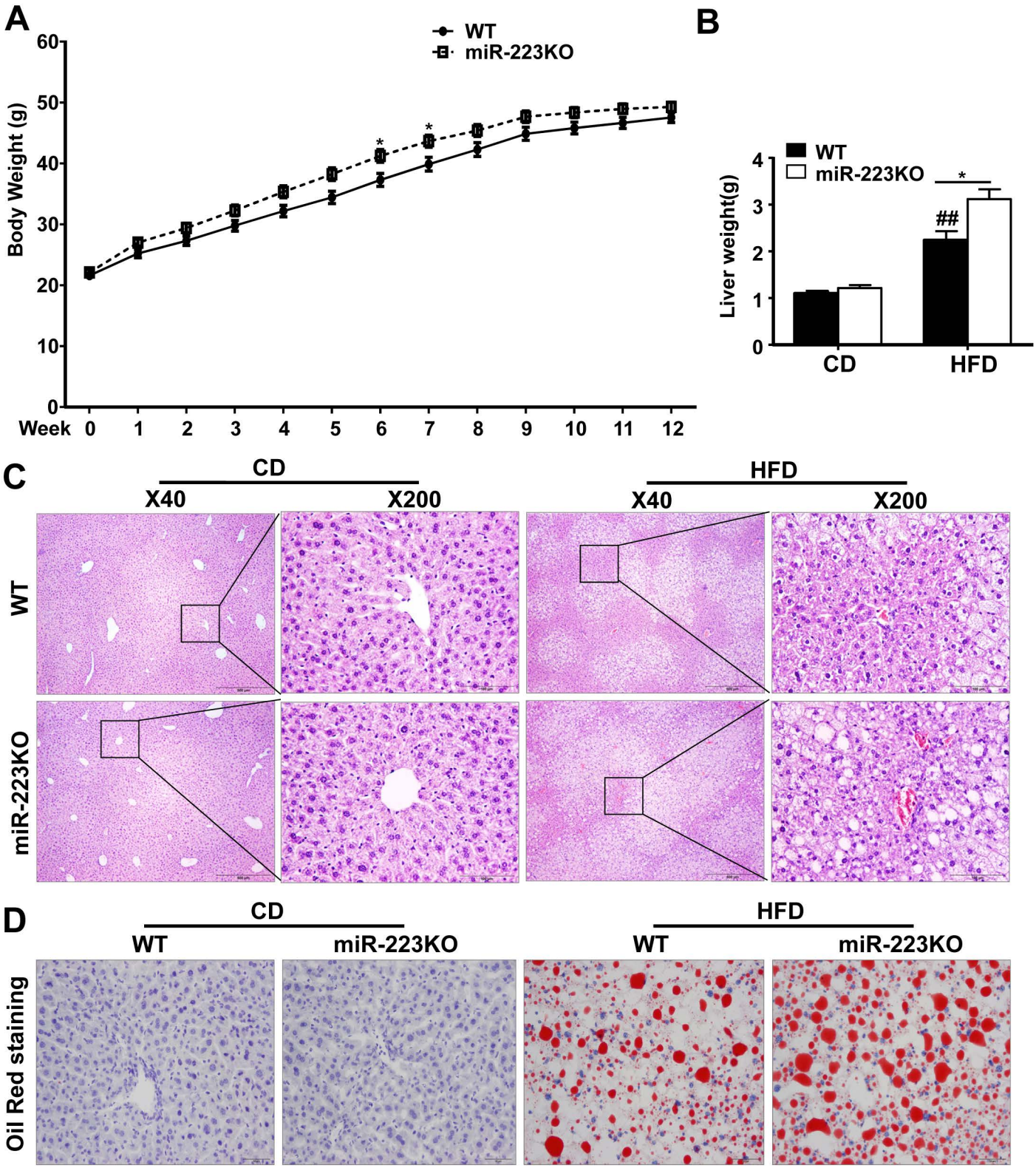

Supporting Fig. S2. miR-223KO are more susceptible to HFD-induced steatosis. WT and miR-223KO mice were fed with a HFD or CD for 3 months. Liver tissue samples were collected. (A) The body weight of WT and miR-223KO mice was measured. (B) Liver weight was measured. (C) Representative images of H&E staining of liver tissue sections were shown. (D) Representative images of Oil Red staining of liver tissue sections were shown. Values represent means ± SEM (n=5-10). $^{*}P< 0.05$ in comparison with WT HFD group; $^{\#\#}P<0.01$ in comparison with WT CD group.

Supporting Fig. S3A-D

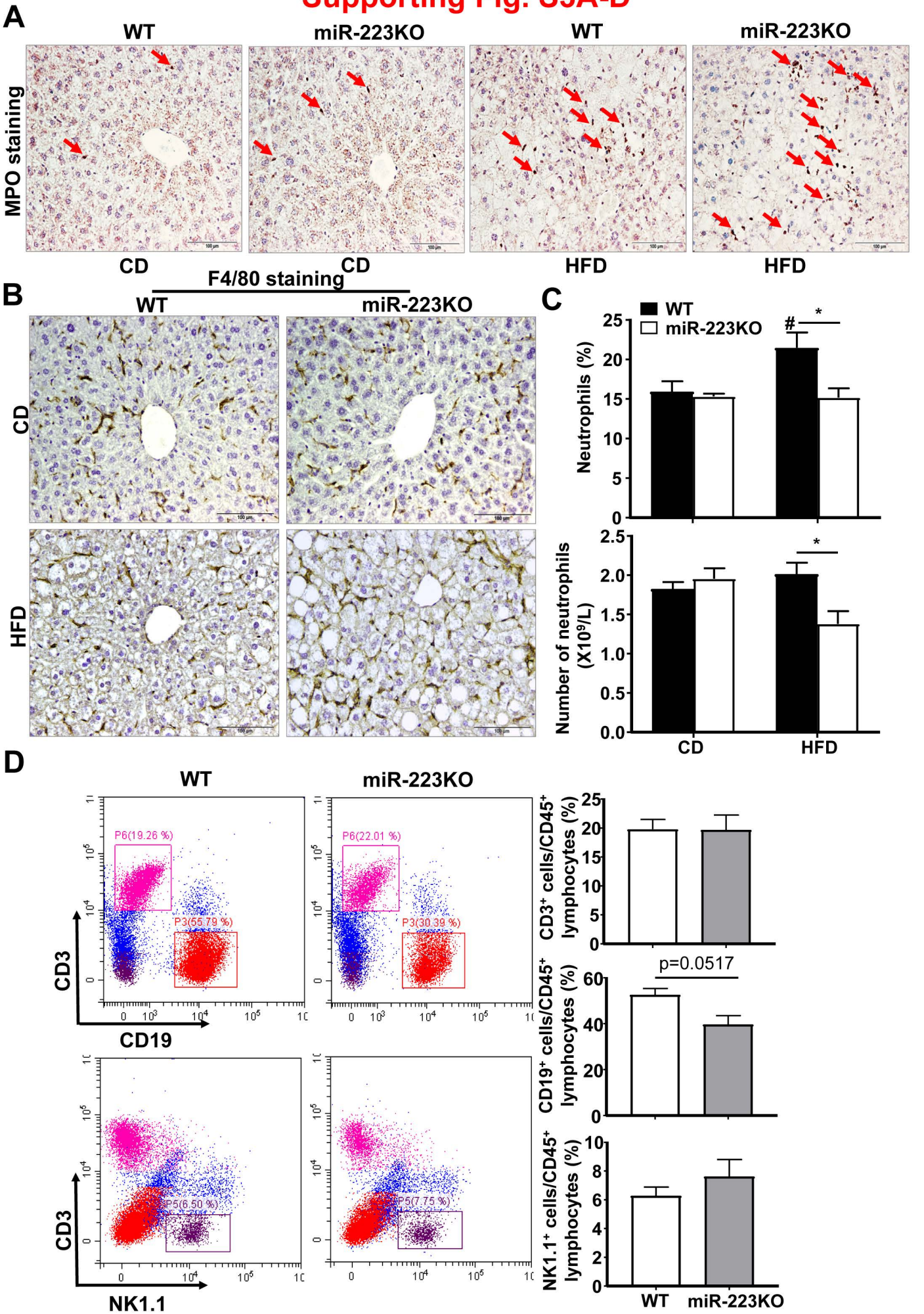

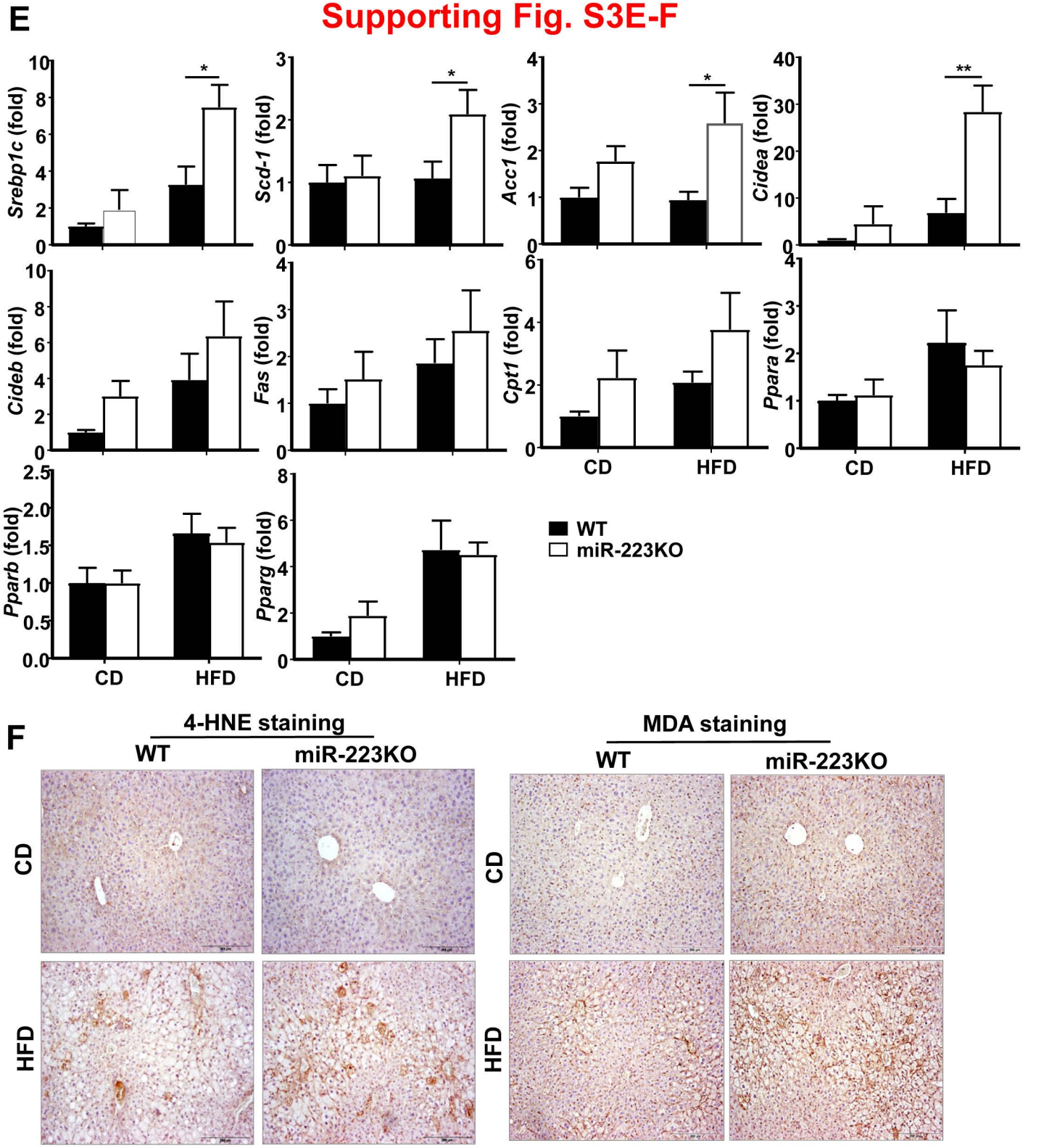

Supporting Fig. S3. miR-223KO mice are more susceptible to HFD-induced inflammation and ROS production compared with WT mice. WT and miR-223KO mice were fed a HFD or CD for 3 months. Liver tissue samples were collected. (A, B) Representative immunostaining of MPO and F4/80. Arrows indicate MPO^+ cells. (C) Percentage and number of circulating neutrophils. (D) Representative of CD3 and CD19 staining of liver tissue sections were shown. Quantification of $CD3^+$ and $CD19^+$ cells per field was quantified. Arrows indicate $CD3^+$ cells (E) RT-qPCR analyses of several steatogenesis genes. (F) Representative 4-hydroxynonenal (HNE) and malonaldehyde (MDA) staining of liver tissue sections were shown. Values represent means ± SEM (n=5-10). $^{**}P<0.01$ in comparison with WT HFD group; $^{\#\#\#}P<0.001$ in comparison with WT CD group.

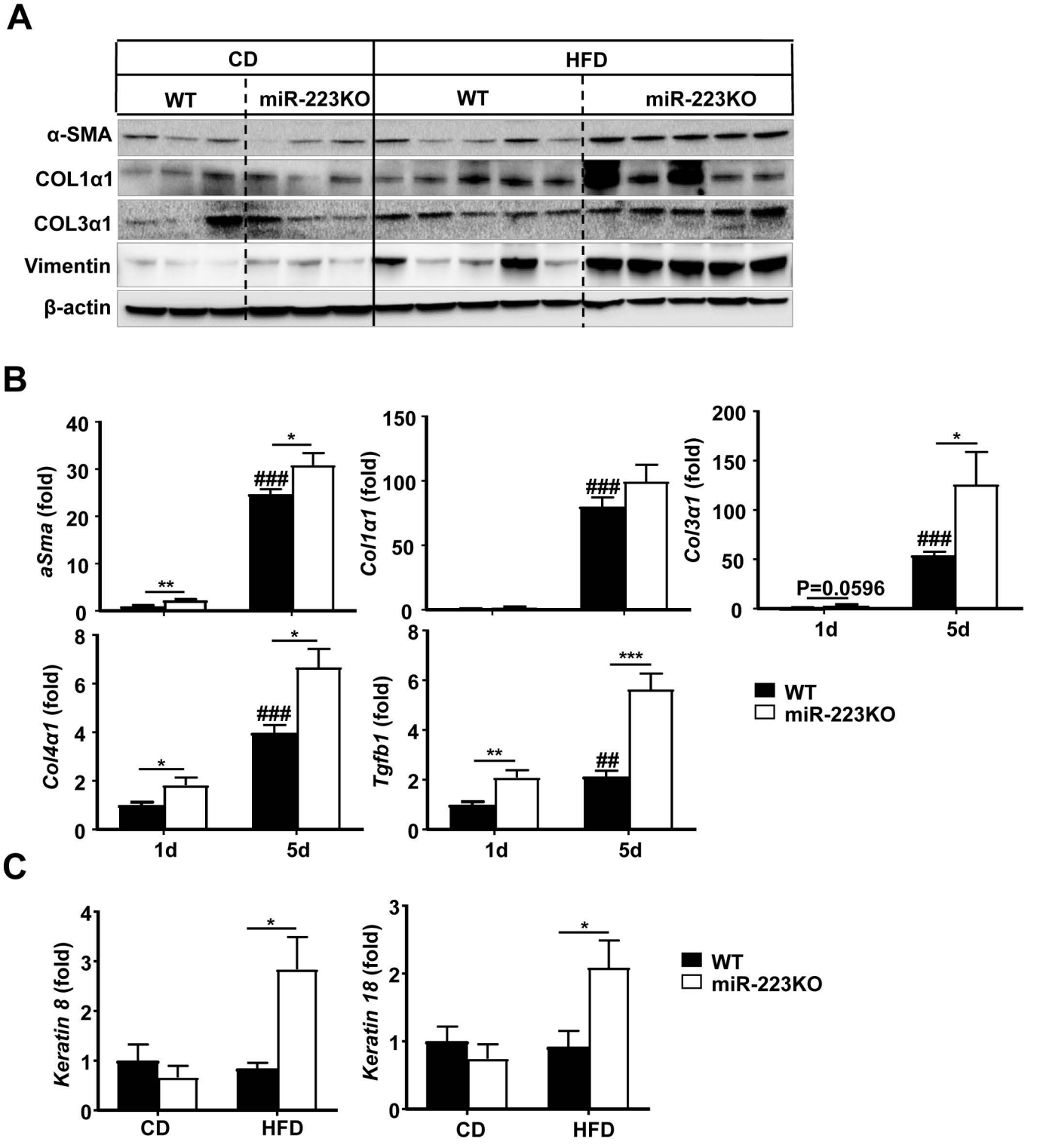

Supporting Fig. S4. HFD feeding for 3 months upregulates fibrogenic proteins and Mallory-Denk bodies-associated genes in miR-223KO mice. (A) WT and miR-223KO mice were fed a HFD or CD for 3 months. Liver tissue samples were collected. Western blotting analyses of fibrogenic genes. (B) Hepatic stellate cells were isolated from WT and miR-223KO mice (without HFD feeding), and cultured for 1d or 5d, followed by RT-qPCR analyses of fibrogenic genes. (C) The samples from Panel A were subjected to RT-qPCR analyses of hepatic *Keratin 8* and *Keratin 18*. Values represent means ± SEM (n=5-10). $^{*}P< 0.05$, $^{***}P<0.001$ in comparison with WT HFD groups. $^{\#\#}P< 0.01$, $^{\#\#\#}P<0.001$ in comparison with WT CD groups.

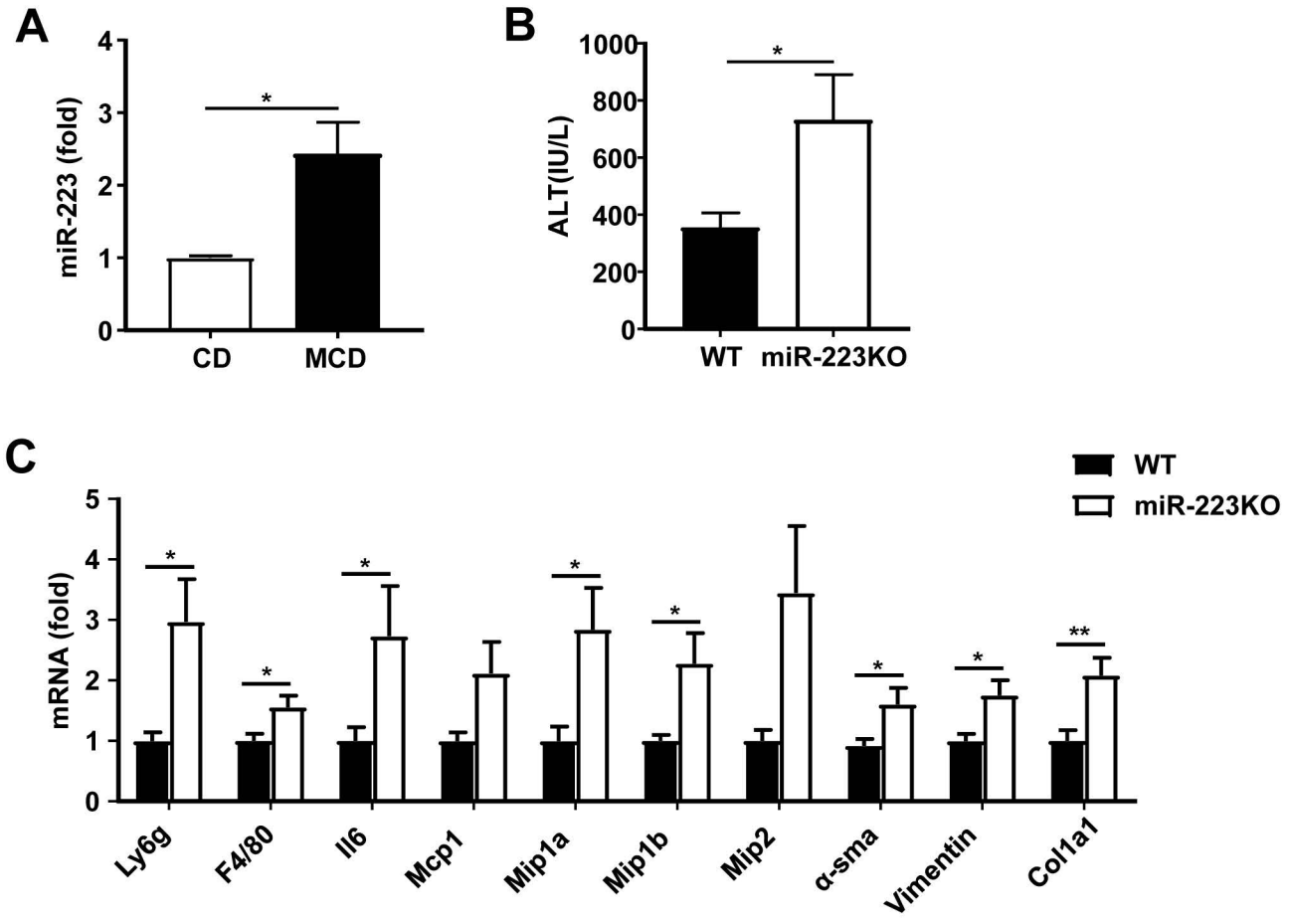

Supporting Fig. S5. miR-223KO mice are more susceptible to MCD-induced NASH. WT and miR-223KO mice were fed a MCD or the MCD control diet (CD) for 4 weeks. Serum and liver tissue samples were collected. (A) RT-qPCR analyses of liver miR-223 levels. (B) Serum ALT levels. (C) RT-qPCR analyses of hepatic inflammatory and fibrogenesis genes. Values represent means ± SEM (n=6-10). $^{*}P< 0.05$, $^{**}P< 0.01$ as indicated.

A

Top Diseases and Bio Functions	
Diseases and Disorders	#Molecules
Cancer	390
Organismal Injury and Abnormalities	397
Inflammatory Response	57

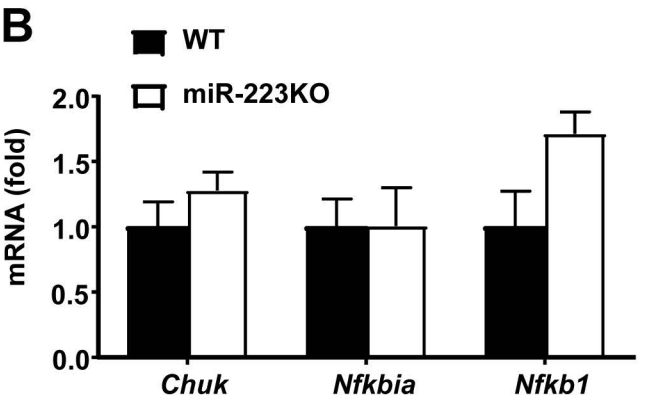

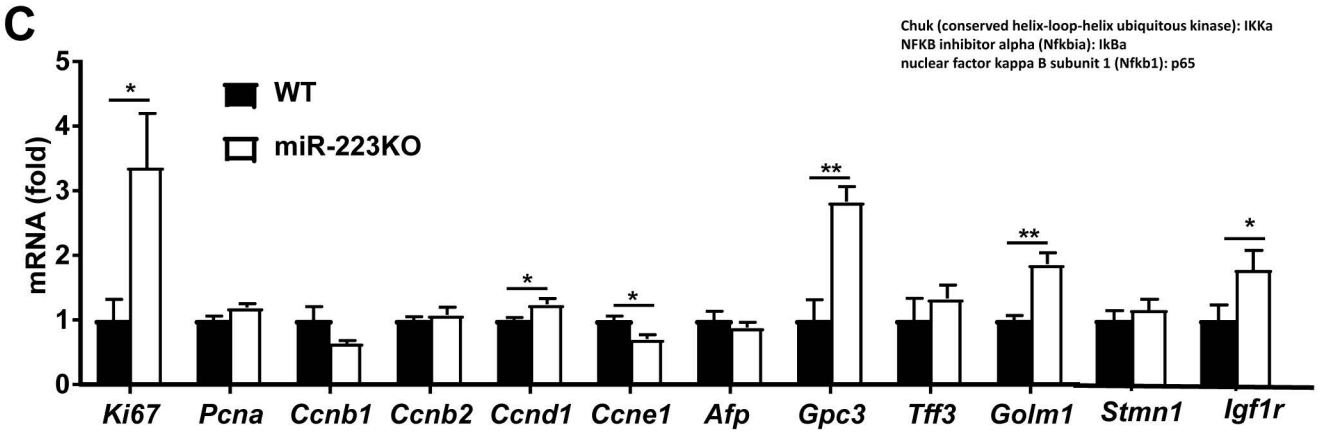

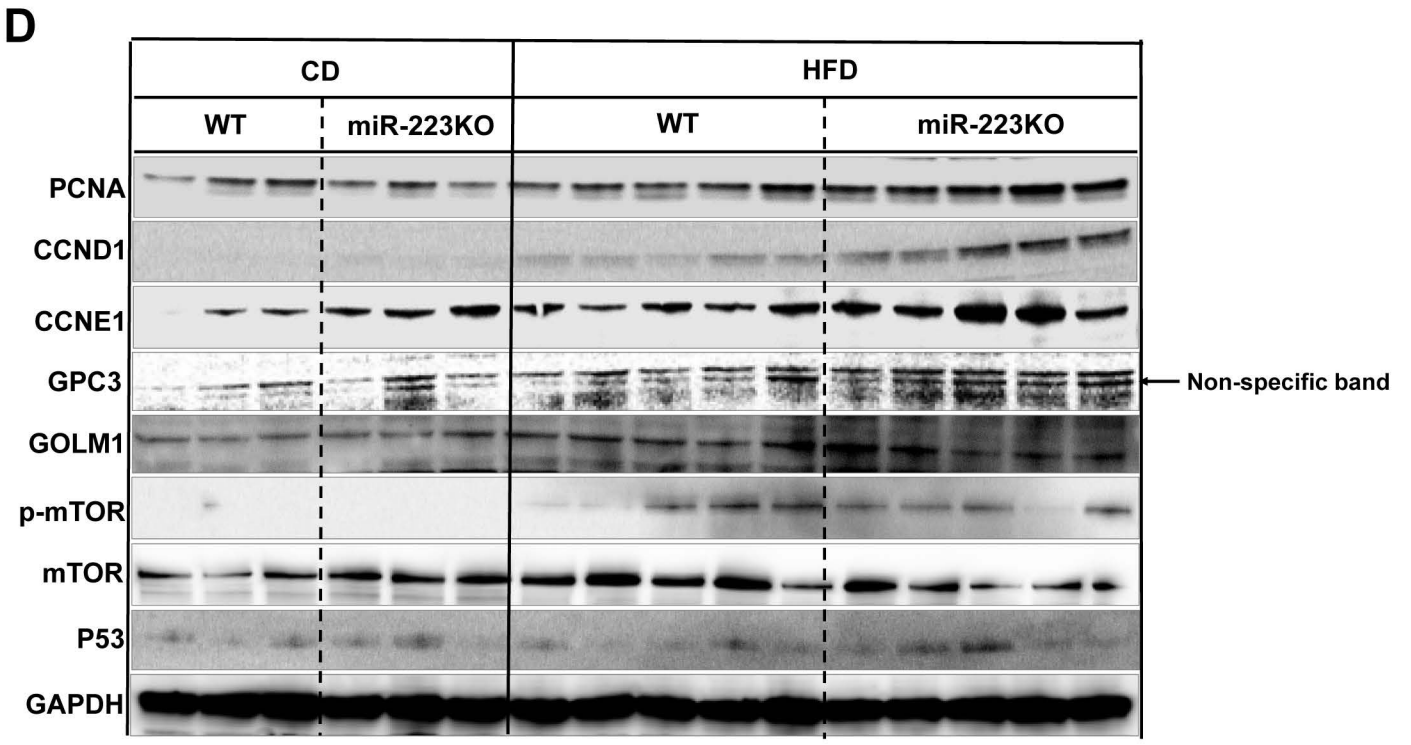

Supporting Fig. S6. The expression of hyperproliferation-related genes are dysregulated in miR-223KO mice after HFD feeding for 3 months. WT and miR-223KO mice were fed a HFD or CD for 3 months. Liver tissue samples were collected, and then subjected to microarray analysis. (A) Ingenuity pathway analyses (IPA) of top diseases/bio-functions in WT and miR-223KO mice after 3m-HFD feeding. (B, C) Hepatic, NF-kB-related genes, proliferation markers and HCC markers were measured by microarray analysis. (D) Hepatic proliferation and HCC markers were detected by western blotting. Values represent means ± SEM. $^{*}P< 0.05$, $^{**}P< 0.01$ in comparison with WT HFD group.

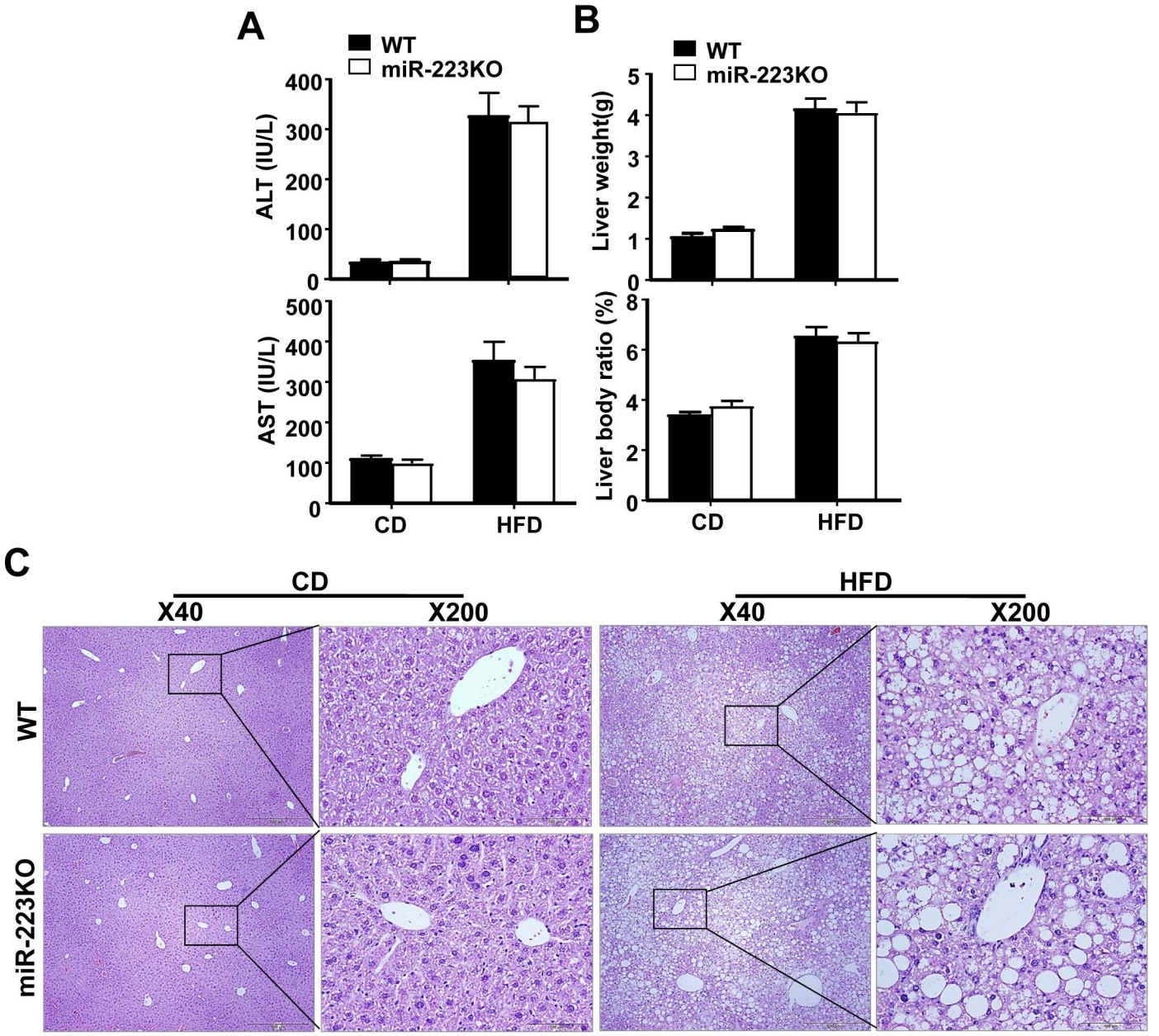

Supporting Fig. S7. miR-223KO mice show similar levels of ALT and steatosis compared with WT mice after HFD feeding for one year. WT and miR-223KO mice were fed a HFD or CD for one year. Liver tissue samples were collected. (A) The levels of ALT and AST were measured. (B) Liver weight and liver body ratio were measured. (C) Representative images of H&E staining of liver tissue sections were shown. Values represent means ± SEM (n=6-21).

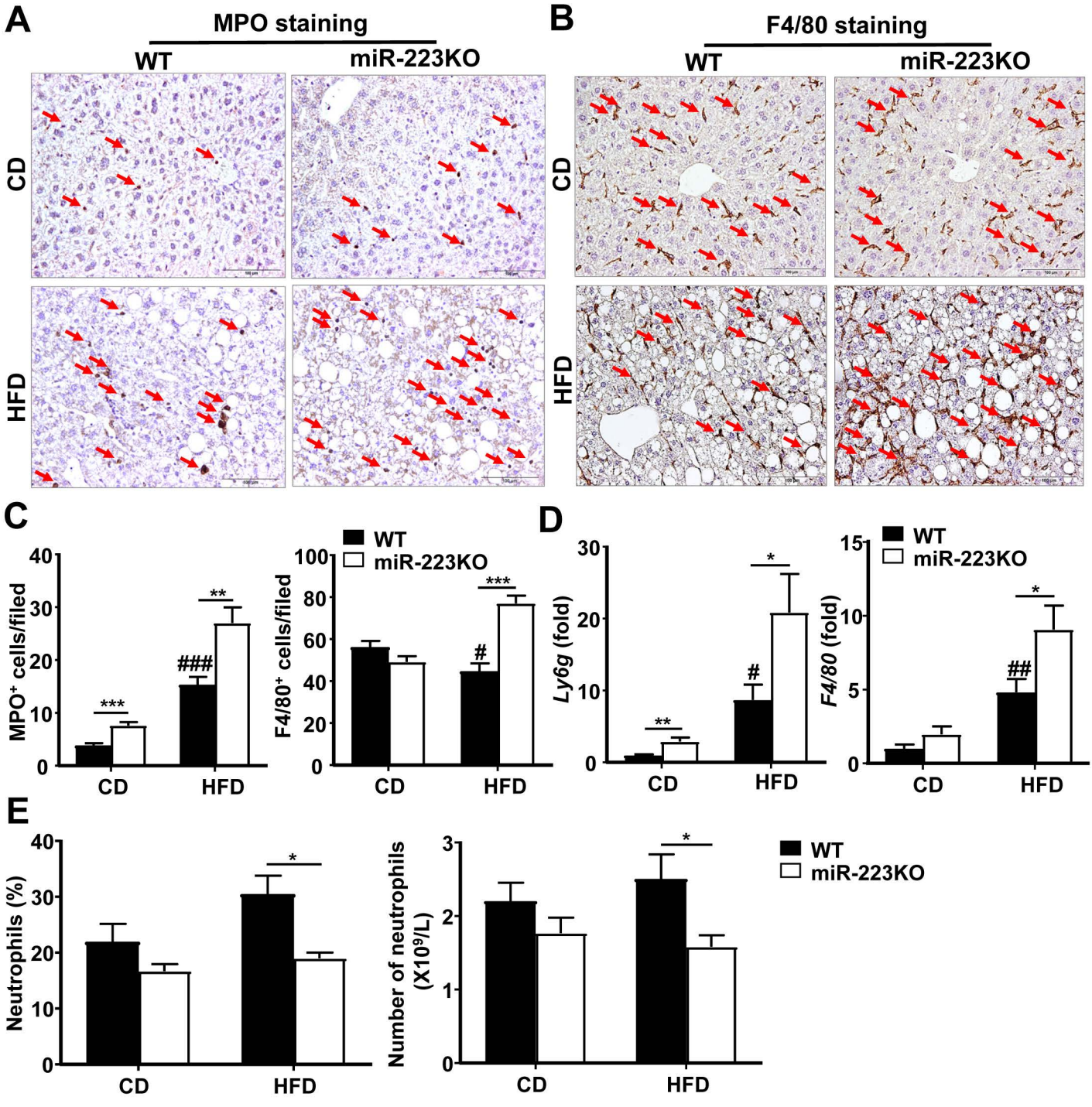

Supporting Fig. S8. miR-223KO mice show greater degree of liver neutrophil and macrophage infiltration, and increased inflammatory response after one-year HFD feeding. WT and miR-223KO mice were fed a HFD or CD for one year. Liver tissue samples were collected. (A, B) Representative MPO and F4/80 staining of liver tissue sections were shown. Arrows indicate MPO$^+$ and F4/80$^+$ cells. (C) MPO$^+$ cells and F4/80$^+$ cells per field were quantified. (D) RT-qPCR analyses of liver *Ly6G* and *F4/80* mRNA. (E) The percentage and number of circulating neutrophils were determined by hematology analyser. Values represent means ± SEM (n=6-21). $^{*}P< 0.05$, $^{**}P< 0.01$, $^{***}P< 0.001$ in comparison with WT HFD groups; $^{\#}P<0.05$, $^{\#\#}P<0.01$, $^{\#\#\#}P<0.001$ in comparison with WT CD groups.

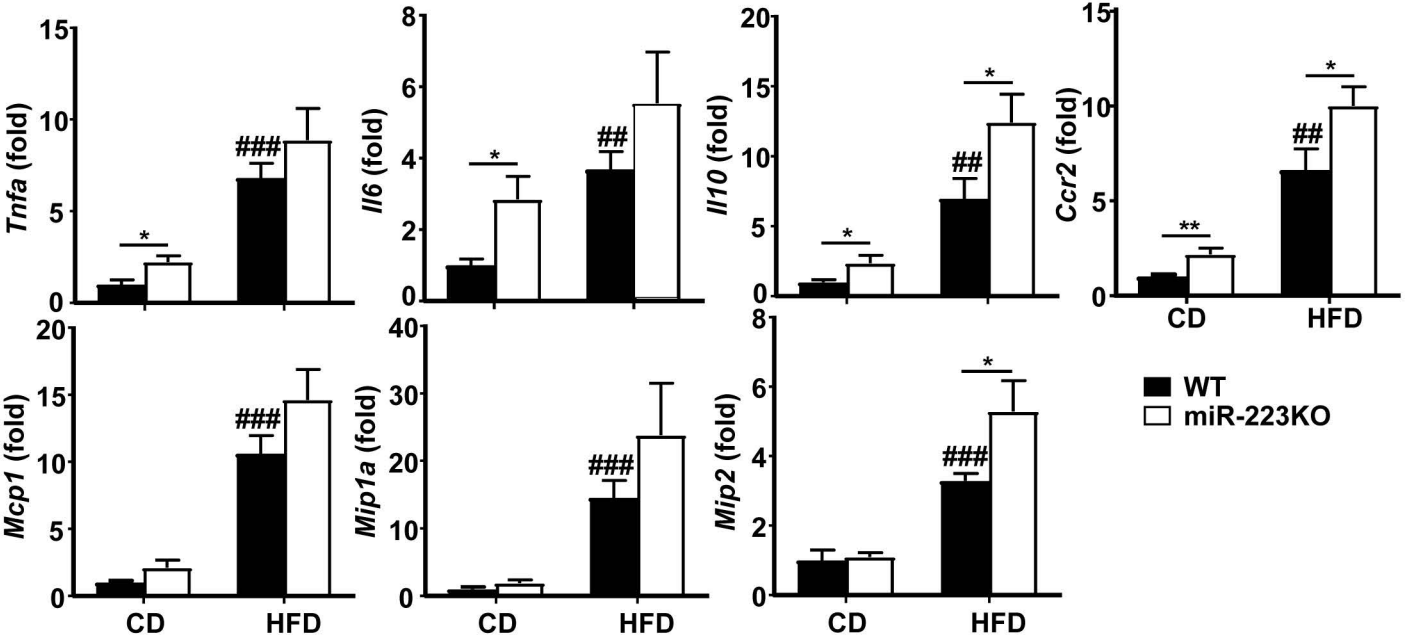

Supporting Fig. S9. miR-223KO mice show greater inflammatory response than WT mice after one-year HFD feeding. WT and miR-223KO mice were fed a HFD or CD for one year. Liver tissue samples were collected. RT-qPCR analyses of several cytokine and chemokine genes. Values represent means ± SEM (n=6-21). $^{*}P< 0.05$, $^{**}P< 0.01$ in comparison with WT STD or HFD group; $^{\#\#}P<0.01$, $^{\#\#\#}P<0.001$ in comparison with WT CD group.

Supporting Fig. S10

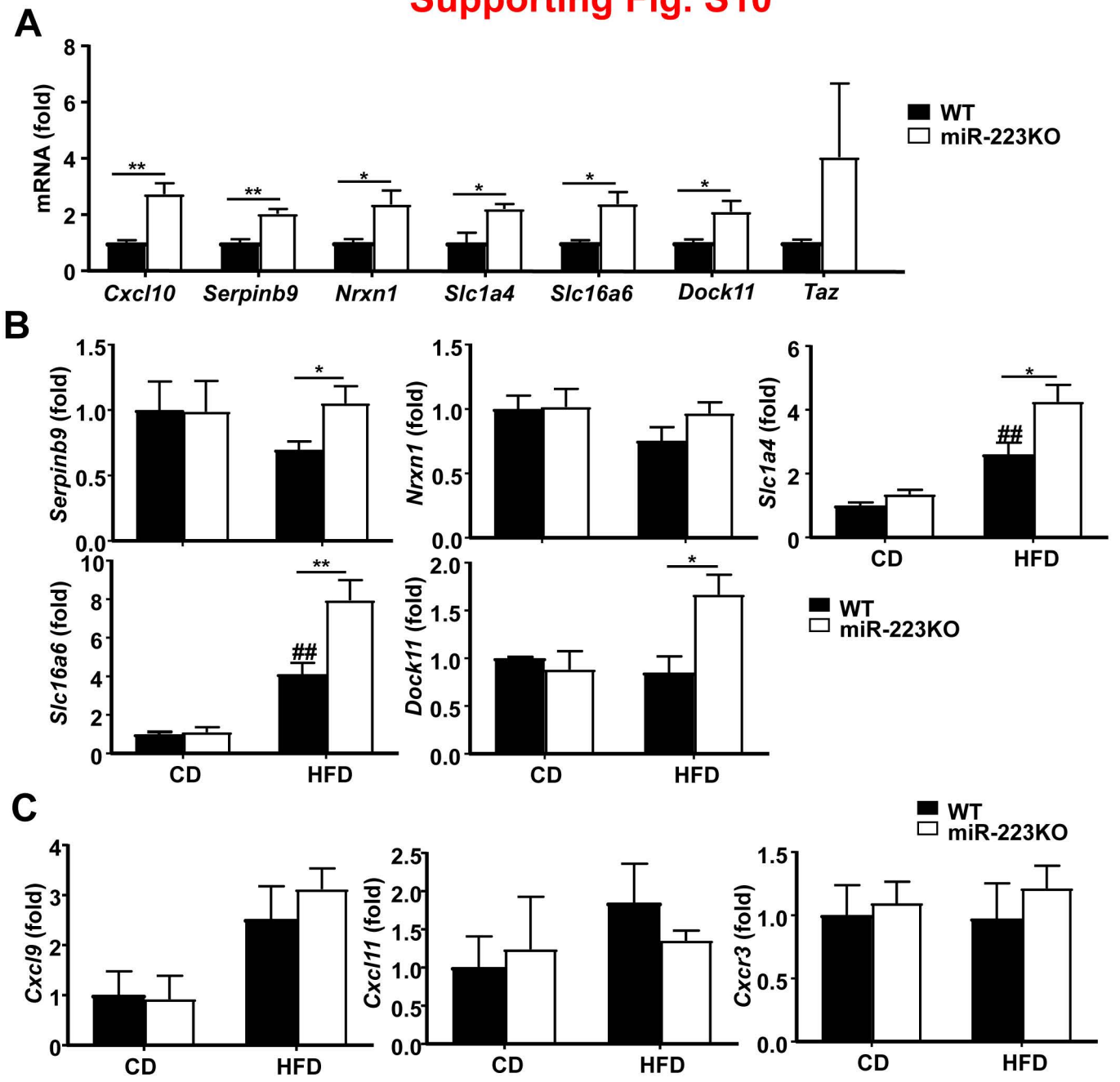

Supporting Fig. S10. The levels of potential miR-223 target genes in WT and miR-223KO mice after 3m-HFD feeding. (A, B) The levels of potential miR-223 target genes were obtained from our microarray data (panel A) and confirmed by RT-qPCR (panel B). (C) RT-qPCR analyses of *Cxcl9*, *Cxcl11* and *Cxcr3*. Values represent means ± SEM (n=5-10). $^{*}P<0.05$, $^{**}P<0.01$ in comparison with WT HFD group; $^{\#\#}P<0.01$ in comparison with WT CD group.

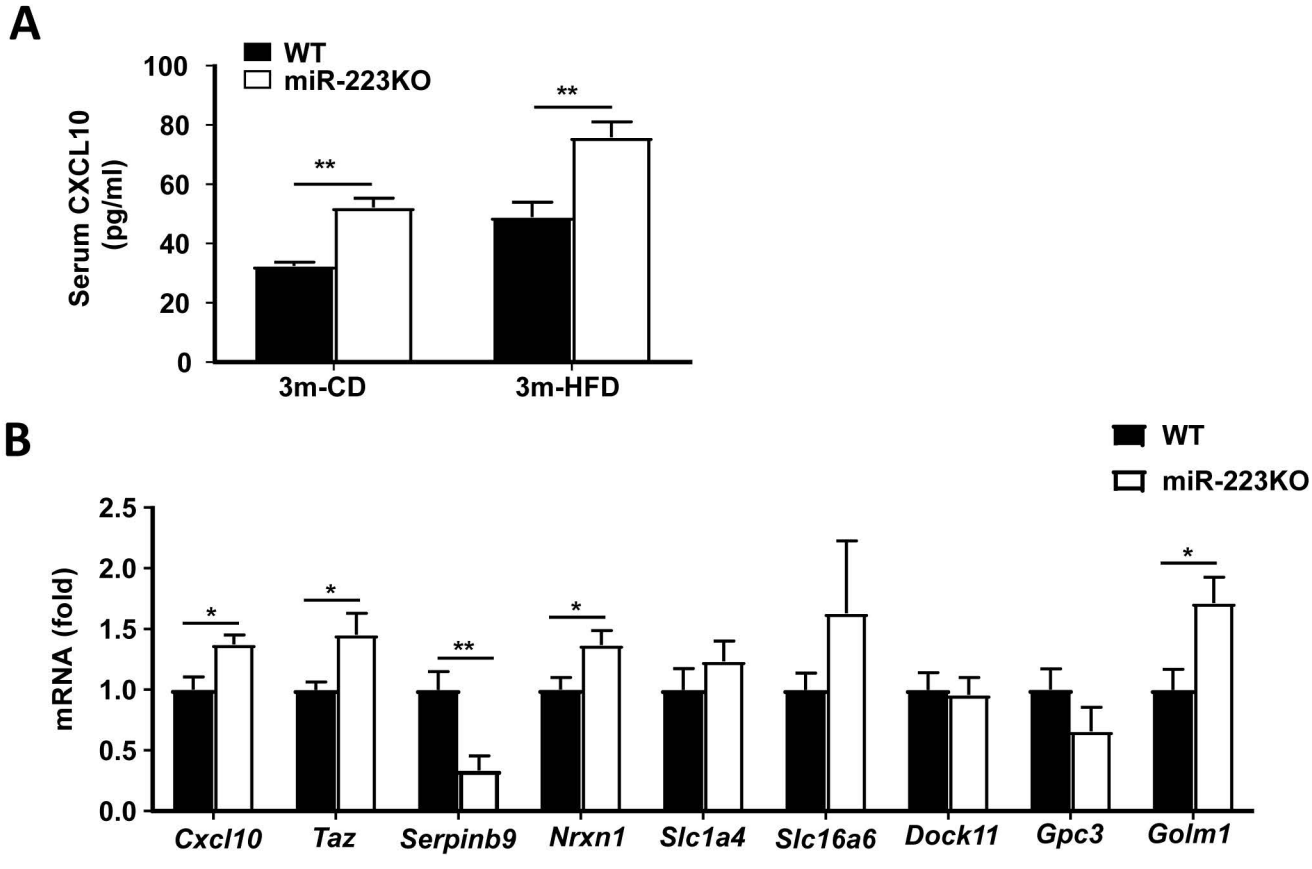

Supporting Fig. S11. (A) miR-223KO mice are associated with higher serum levels of CXCL10 than WT mice after 3m-HFD feeding. WT and miR-223KO mice were fed a HFD or CD for three months. Serum levels of CXCL10 were measured. Values represent means ± SEM (n=6-21). $^{**}P<0.01$. **(B) miR-223KO mice are more susceptible to MCD-induced *Cxcl10* and *Taz* expression.** WT and miR-223KO mice were fed a MCD for 4 RT-qPCR analyses of potential miR-223 targeted genes. Values represent means ± SEM (n=5-10). $^{*}P< 0.05$, $^{**}P<0.01$.

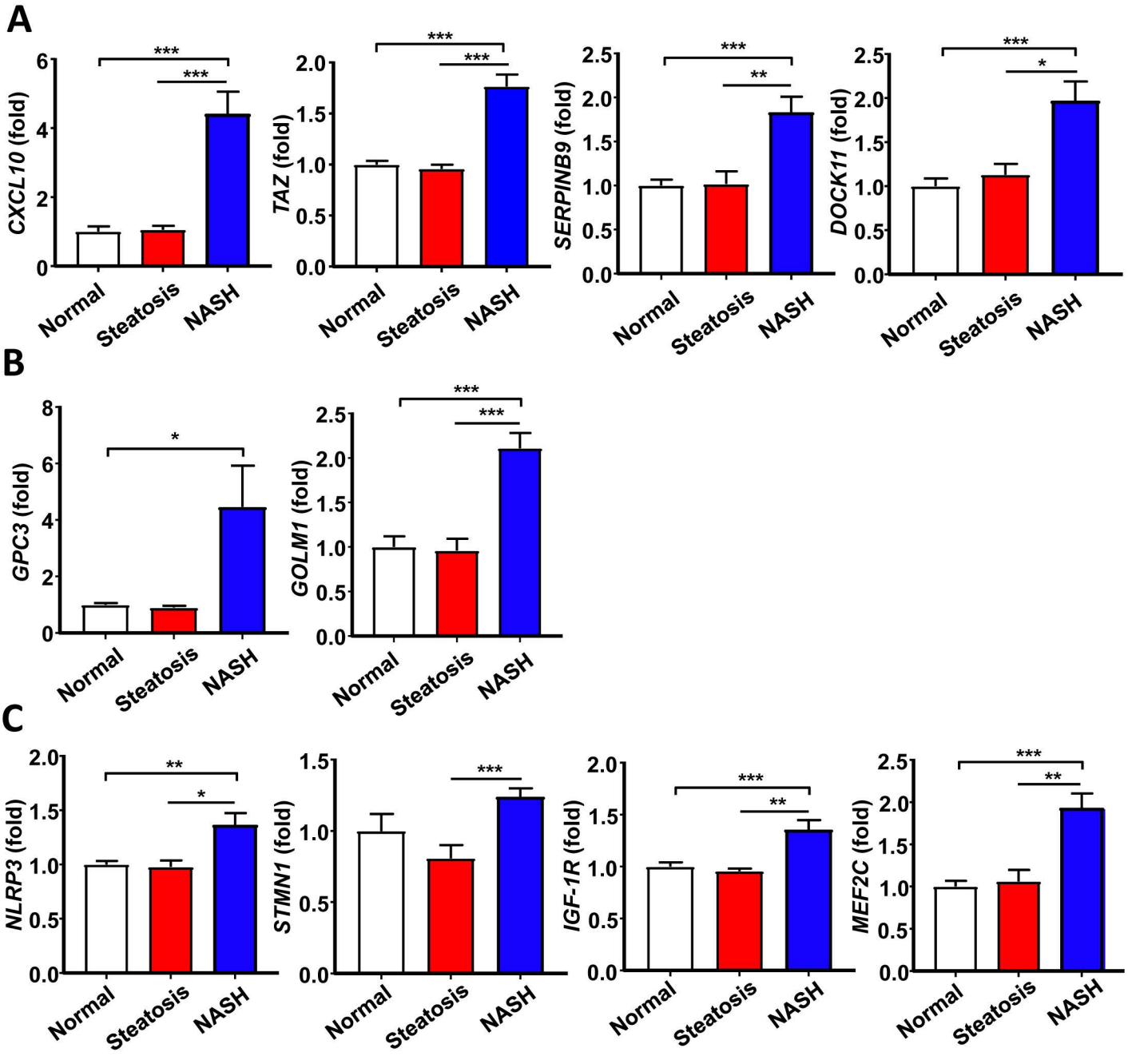

Supporting Fig. S12. Several potential miR-223 targets of liver cancer-related genes are significantly upregulated in NASH patients. The samples were diagnosed as normal (n=19), steatosis (n=10), NASH (n=16). (A) Several potential targets of miR-223 were measured by microarray analysis from published microarray data (the accession number E-MEXP-3291 [http://www.webcitation.org/5zyojNu7T]). (B) Cancer-related genes were measured by microarray analysis. (C) Several proven miR-223 targeted genes were measured by microarray analysis. Values represent means ± SEM. $^{*}P< 0.05$, $^{**}P< 0.01$, $^{***}P< 0.001$.

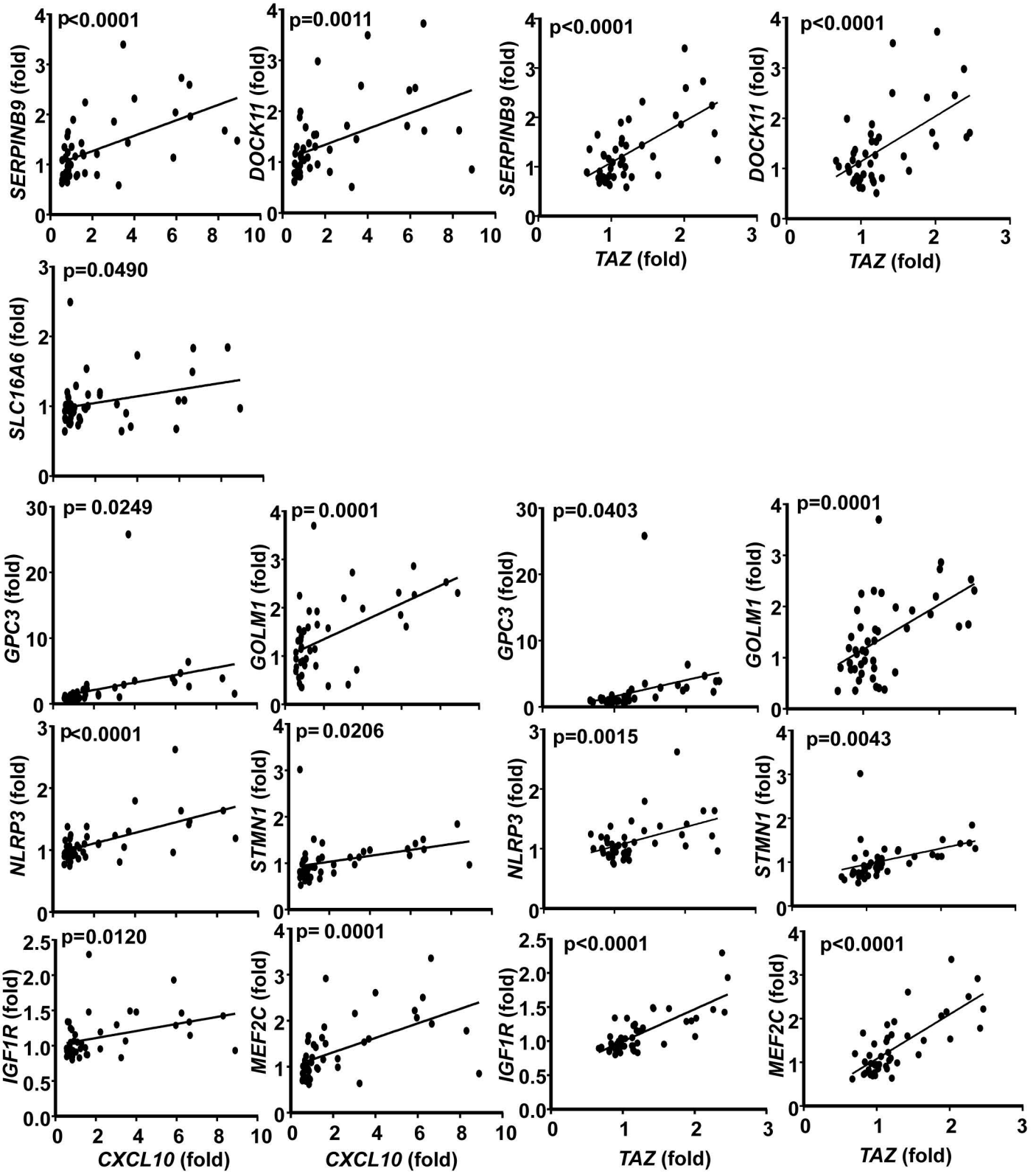

Supporting Fig. S13. Several potential and proven miR-223 targeted genes positively correlate with *CXCL10* or *TAZ expression* in NASH patients. Microarray analysis of normal (n=19), steatosis (n=10), NASH (n=16) was obtained from published microarray data (the accession number E-MEXP-3291 [http://www.webcitation.org/5zyojNu7T]). Several potential and proven miR-223 targeted genes positively correlated with *CXCL10* or *TAZ* in NASH patients. P value is indicated.

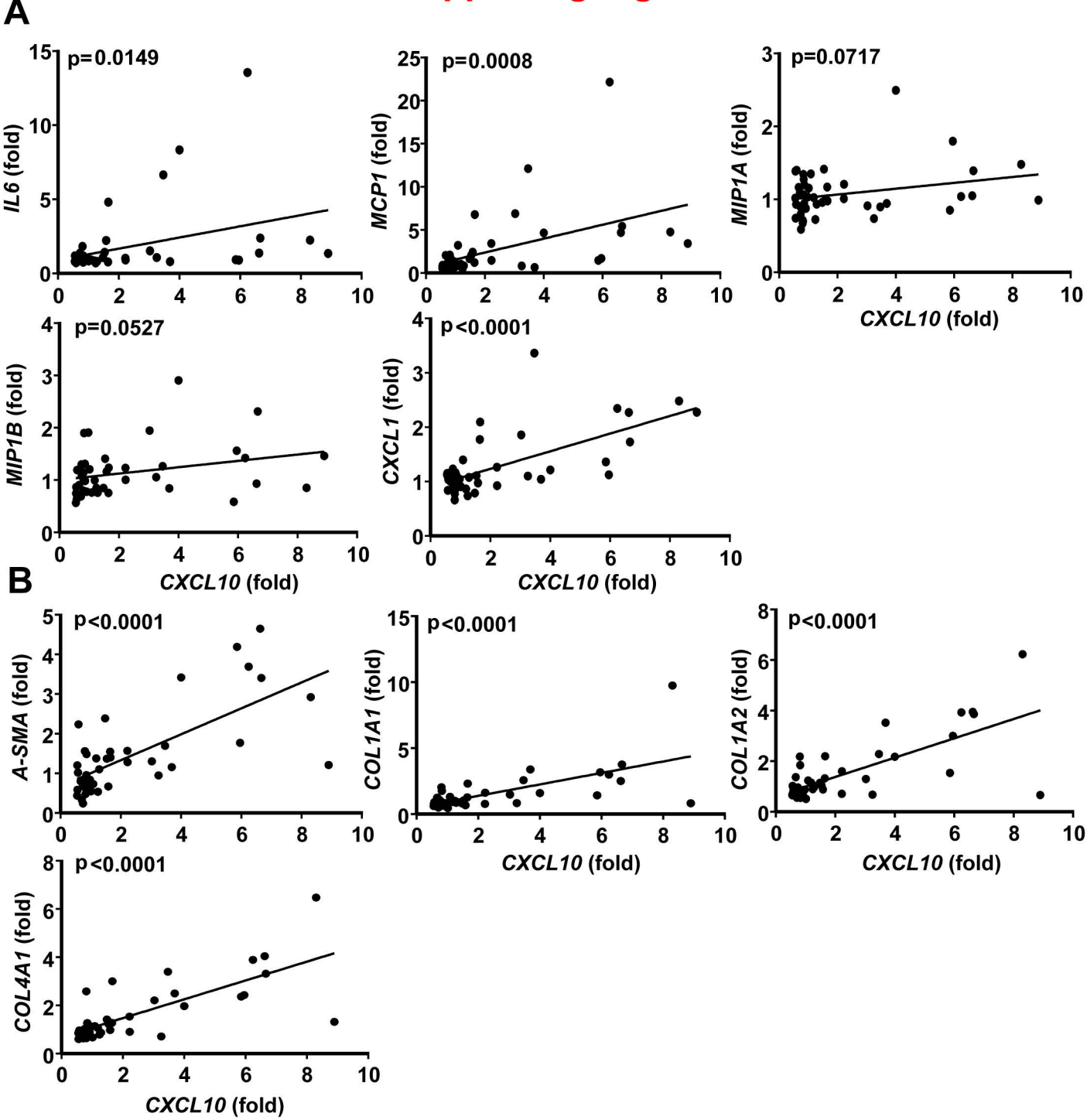

Supporting Fig. S14. Several cytokine and chemokine genes and fibrogenesis genes positively correlate with *CXCL10 expression* in NASH patients. Microarray analysis of normal (n=19), steatosis (n=10), NASH (n=16) was obtained from published microarray data (the accession number E-MEXP-3291 [http://www.webcitation.org/5zyojNu7T]). Several cytokine and chemokine genes and fibrogenic genes positively correlate with *CXCL10* in NASH patients. P value is indicated.

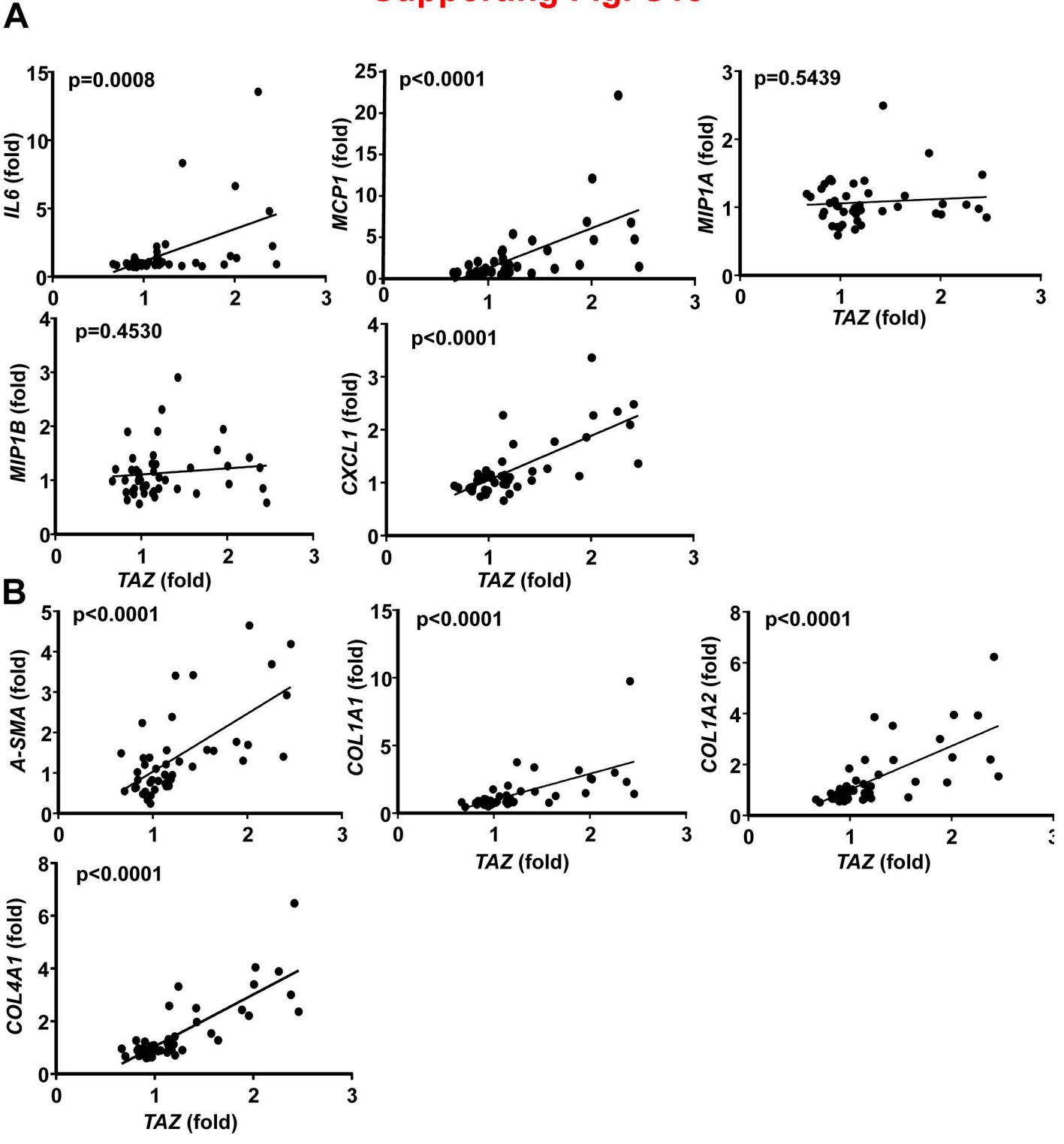

Supporting Fig. S15. Several cytokine and chemokine genes and fibrogenesis genes positively correlate with *TAZ expression* in NASH patients. Microarray analysis of normal (n=19), steatosis (n=10), NASH (n=16) was obtained from published microarray data (the accession number E-MEXP-3291 [http://www.webcitation.org/5zyojNu7T]). Several cytokine and chemokine genes and fibrogenic genes positively correlate with *TAZ* in NASH patients. P value is indicated.